Dynamic imaging of dendritic cell extension into the small bowel lumen in response to epithelial cell TLR engagement

Marcello Chieppa,[1] Maria Rescigno,[2] Alex Y.C. Huang,[1] and Ronald N. Germain[1]

[1]Lymphocyte Biology Section, Laboratory of Immunology, National Institute of Allergy and Infectious Diseases (NIAID), National Institutes of Health (NIH), Bethesda, MD 20892
[2]Department of Experimental Oncology, European Institute of Oncology, 20141 Milan, Italy

Cells lining the gastrointestinal tract serve as both a barrier to and a pathway for infectious agent entry. Dendritic cells (DCs) present in the lamina propria under the columnar villus epithelium of the small bowel extend processes across this epithelium and capture bacteria, but previous studies provided limited information on the nature of the stimuli, receptors, and signaling events involved in promoting this phenomenon. Here, we use immunohistochemical as well as dynamic explant and intravital two–photon imaging to investigate this issue. Analysis of CD11c–enhanced green fluorescent protein (EGFP) or major histocompatibility complex CII–EGFP mice revealed that the number of trans-epithelial DC extensions, many with an unusual "balloon" shape, varies along the length of the small bowel. High numbers of such extensions were found in the proximal jejunum, but only a few were present in the terminal ileum. The extensions in the terminal ileum markedly increased upon the introduction of invasive or noninvasive *Salmonella* organisms, and chimeric mouse studies revealed the key role of MyD88–dependent Toll-like receptor (TLR) signaling by nonhematopoietic (epithelial) elements in the DC extension response. Collectively, these findings support a model in which epithelial cell TLR signaling upon exposure to microbial stimuli induces active DC sampling of the gut lumen at sites distant from organized lymphoid tissues.

CORRESPONDENCE
Ronald N. Germain:
rgermain@nih.gov

Abbreviations used: BB, balloon body; EGFP, enhanced GFP; PAMP, pathogen-associated molecular pattern; PG, peptidoglycan; SNARF, carboxylic acid acetate succinimidyl ester; TLR, Toll-like receptor.

The gastrointestinal tract is a major site of host invasion by pathogenic organisms. Indeed, even during periods of health, the gut lumen is the site of a large population of bacteria, which under normal conditions contribute to the viability of the host (1, 2). However, this balanced state of coexistence is not autonomous but actively maintained by local protective mechanisms such as defensins (3) and ongoing adaptive immune responses that help ensure that the commensal bacteria remain resident on the lumenal side of the gut lining (4). Defects in these protective responses, for example, sIgA deficiency, can result in breach of this barrier, with potential consequences ranging from septicemia to inflammatory bowel disease (5).

A.Y.C. Huang's present address is Division of Pediatric Hematology/Oncology, Rainbow Babies and Children's Hospital, Case Western Reserve University School of Medicine, Cleveland, OH 44106.

The online version of this article contains supplemental material.

Both T-dependent and T-independent B cell antibody production contribute to ongoing anti-commensal immunity as well as to acute responses against pathogenic organisms. Antigen associated with DCs plays a key role not only in the well-recognized activation of T cells that can provide help for B cells, but also in the direct presentation of antigen to B cells (5–9). Thus, the mechanisms by which gut-localized DCs acquire antigenic information are of significance in both the maintenance of homeostasis and in the development of protective immunity to pathogens.

Specialized cells (M cells) situated in the dome region of Peyer's patches are a major route for the transfer of antigen, including intact bacteria and viruses, from the gut lumen to underlying DCs (10, 11). Recent studies suggest that M cells also exist in villi where they may contribute to the transfer of organisms from bowel lumen to lamina propria DCs

(12, 13). Under nonpathogenic conditions, these antigen–laden DCs can interact with associated T and B lymphocytes to generate a noninflammatory immune response biased through local signals such as TGFβ (14, 15) and in humans, TSLP (16). However, during noncommensal bacterial invasion, signals provided directly or indirectly by these organisms can alter the differentiation of freshly recruited DCs and deviate the immune response to a more inflammatory character (16).

In the past few years, another mode of antigen uptake within the gastrointestinal tract has been reported. In vitro studies using a model epithelial cell line first revealed the capacity of DCs on the basolateral (ablumenal) side of the epithelium to extend processes across the tight junctions between these cells and capture bacteria from the apical (lumenal) side (17, 18). Remarkably, this extension occurred without compromising the integrity of the epithelial barrier, apparently as a result of the creation of a tight junction–like structure between the dendrites and the contiguous epithelial cells. Immunohistochemical studies with gut tissue provided initial limited evidence that such DC extensions existed in vivo, a result confirmed and extended by more recent high resolution static imaging studies (13, 19). These latter papers used fractalkine receptor (CX3CR1)-driven expression of enhanced GFP (EGFP) to visualize the gut DC population and suggested that CX3CL1 may play a role in guiding extension of this DC subset across the epithelium. These experiments also showed that the EGFP-expressing DCs acquired microorganisms from the gut lumen when fractalkine signaling was present, although the study by Vallon-Eberhard et al. (13) did not find the extensions to be required for such trans-epithelial transport.

In both of these previous analyses, exposure of the small bowel lumenal surface to bacterial or fungal products was shown to increase the extent of trans-epithelial DC extension, but no information was obtained on the mechanism of this induced response. Likewise, the question of whether the steady-state level of DC trans-epithelial extension is a constitutive activity of the DCs or sustained by stimuli from commensal flora has not been addressed, although the addition of commensal organisms to the gut lumen under defined conditions has been shown to increase the number of such extensions (19). Here, we explore this issue of regulated trans-epithelial extension of processes by lamina propria DCs using dynamic explant and intravital imaging methods to visualize these events under a variety of experimental conditions. We find that these DC-derived processes, which often have an unusual spherical ("balloon body") shape and whose frequency varies along the small bowel length, are generated in large measure in response to MyD88-dependent signaling by a subset of Toll-like receptors (TLRs) expressed by nonhematopoietic (epithelial) cells. Our findings strongly support the previously proposed model of gastrointestinal lumen sampling by DCs and provide new insight into the location and structural characteristics of the trans-epithelial extensions as well as initial characterization of the signals inciting this sampling of the gut lumenal flora.

RESULTS
Differences in the frequency of lamina propria DC extensions along the length of individual villi and of the small bowel in normal mice

Two high resolution microscopic studies have documented the presence of abundant trans-epithelial DC extensions in the small bowel of mice on the C57BL/6 background (13, 19). To determine the optimal site(s) for dynamic imaging of such extensions, we first conducted a similar static imaging analysis using explants from distinct subregions of the small bowel. Previous studies examined DCs marked by EGFP expression under the control of the CX3CR1 gene regulatory region. Here, we studied small bowel segments from mice whose DCs expressed a fluorescent MHC class II molecule in which the Aβ[b] chain is covalently linked to EGFP as a consequence of gene targeting (MHC CII-EGFP; reference 20) or from mice whose DCs expressed cytoplasmic EGFP under control of the CD11c promoter-enhancer region (CD11c-EGFP; reference 21). In the case of the tissues from the Aβ[b] gene-targeted animals, the identity of the fluorescent cells as DCs was confirmed using RAG-2^{−/−} animals that lack B cells and by FACS analysis of dissociated tissue (Fig. S1, available at http://www.jem.org/cgi/content/full/jem.20061884/DC1).

A representative three-dimensional reconstruction of a small bowel imaging dataset is shown in Fig. 1 A and Video S1, which is available at http://www.jem.org/cgi/content/full/jem.20061884/DC1. In agreement with previous findings, each villus in this image from the ileum 30 cm distal to the stomach had several DC extensions visible on the lumenal side of the epithelium. Two features were notable in these imaging data. First, the extensions were more frequent in the apical region of the villi and rarer near the basal regions close to crypts (Fig. 1 B and Video S2), although no difference in DC numbers was detected along the length of the villi. Second, the extensions had an unusual shape, most often being nearly spherical rather than finger-like (Fig. 1, A and C), giving rise to what we call balloon bodies (BBs). This shape was seen using several distinct surgical preparations of the bowel segment and with various media bathing the tissue during imaging (unpublished data), but because the majority of the residual bowel contents and mucus must be removed for successful imaging in all cases, we cannot be certain that this shape is adopted by DC extensions under truly physiological conditions (see Discussion). Globular structures were also noted in at least a subset of the trans-epithelial extensions of CX3CR1-EGFP cells imaged by others (13, 19). Similar numbers, distribution, and shapes of DC trans-epithelial extensions were seen using CD11c-EGFP or MHC CII-EGFP mice. The common findings using both of these reporter animals make it unlikely that the extensions originate from mucosal macrophages that have been reported to be CD11c^{+} (22).

When the frequency of such trans-epithelial DC extensions was measured along the length of the small bowel, clear regional differences were observed (Fig. 2 A). The extensions were present in substantial number from the jejunum through most of the ileum, with a slightly greater frequency in the
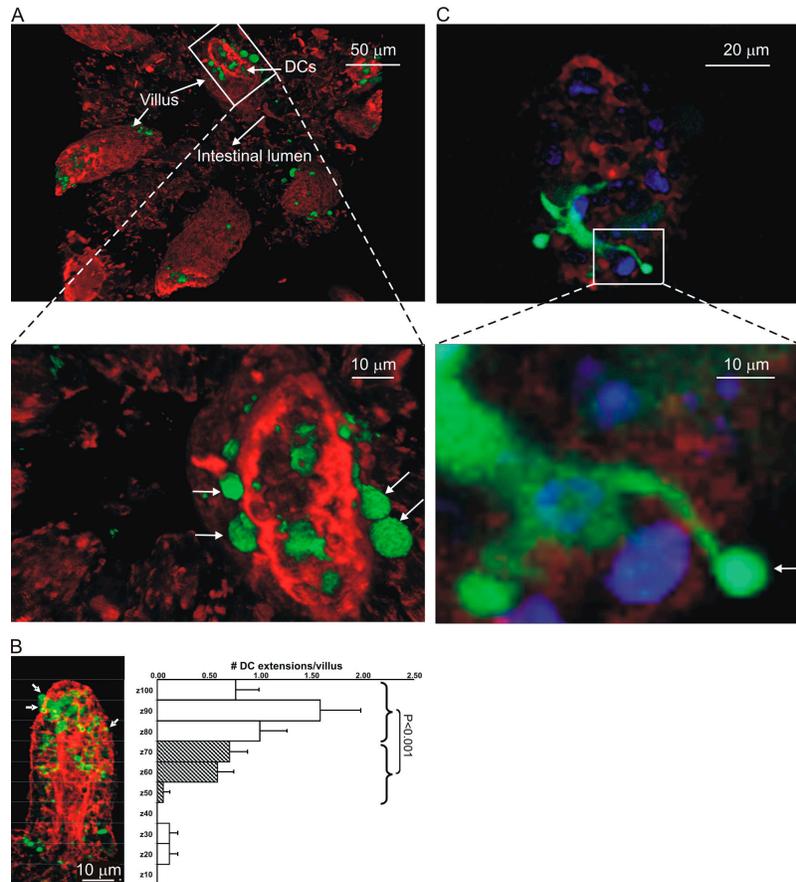
Figure 1. DCs extend through the apical epithelium of villi.
(A) Static two-photon microscopy image of the villi in the peri-cecal region of a CD11c-EGFP mouse given noninvasive *Salmonella* orally 3 h before imaging (top). The image is a three-dimensional reconstruction of 65 serial optical sections (1.5 μm/z-section) comprising a total depth of 97.5 μm. Extensions of DCs (green) into the intestinal lumen can be observed. The surface of the villi was outlined by SNARF-1 staining of the epithelial cells (red). Bar, 25 μm. Boxed region in the top panel is shown in a higher magnification in the bottom panel to better illustrate how DC extensions (green) protrude through the intestinal epithelium (red) into the luminal cavity. The arrows indicate examples of spherical DC extensions into the intestinal lumen (also see Video S1). (B) A representative static image of an ileal villus from an MHC CII-EGFP mouse stained with SNARF-1 to highlight the epithelial cells (red) shows the preferential location of DC extensions (green) near the apical region of the villus (white arrows).

The villus was arbitrarily subdivided in 10 equal compartments from the bottom to the apical region (z = 0 to z = 100), and the average number of DC extensions in each compartment is displayed in the histogram. Values are expressed as the number of DC extensions per villus in the indicated section (mean ± SE). The top regions (z = 70–100; open bars) show a significant difference in the number of DC extensions as compared with the middle and lower parts (z = 40–70; striped bars) of the villi. Also see Video S 2. (C) A single optical z-slice of a villus from the ileum of an MHC CII-EGFP mouse. Epithelial cells are stained with SNARF-1 (red), and the cell nuclei are stained with Hoechst 33342 (blue). The higher magnification in the bottom panel demonstrates a DC extending an MHC CII[+] (green) dendrite through the epithelium. Once reaching the intestinal lumen, the DC dendrite assumes the characteristic shape of a sphere (white arrow).

proximal portion of the latter small bowel segment. However, villi in the terminal 5 cm of the ileum near the cecal region had a very low number of DC extensions in unmanipulated healthy animals. These observations differ from those reported previously using mice expressing EGFP under the control of the CX3CR1 gene regulatory region (13, 19), in which the terminal ileum was found to have the highest density of visualized extensions. Both these earlier reports and ours involve mice on the same genetic background (C57BL/6), making this an unlikely source of the difference. The major distinction between the studies is the method for detecting DCs involving EGFP expression by only the

CX3CR1^{+} subset in the case of the previous reports and a broader analysis involving labeling of all CD11c^{+} or MHC class II^{+} DCs in the present case. The following sections provide evidence that analysis of DC subsets differentially marked by the various reporter constructs may account for these contrasting observations.

Small bowel bacterial content affects the frequency of trans–epithelial DC extension
The variation in the frequency of DC extension both along a villus and the length of the small bowel could reflect either intrinsic properties of the tissue or the impact of exogenous
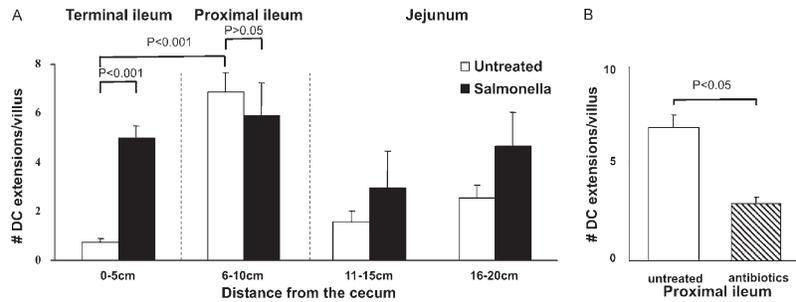
stimuli that actively induce the extension response. A likely source of such exogenous stimuli is the commensal bacteria of the gut, a possibility we examined by treating mice with broad-spectrum antibiotics for 5 d to reduce the bacterial load and then analyzing the distribution and number of DC extensions. This treatment resulted in a significant decrease in the frequency of DC extensions in the proximal regions of the small bowel where they were the most numerous in normal animals (Fig. 2 B). DC protrusions were not completely abrogated, possibly due to the residual bacterial population remaining after antibiotic treatment. In agreement with previous data implicating microbial stimuli in induction of DC extensions, an additional bacterial load consisting of live *Salmonella* administered by gavage led to the appearance of a substantial number of extensions in the peri-cecal region in which such DC processes were typically rare in normal mice (Fig. 2 A). The induction of BBs can be detected 3 h after bacteria gavage. The process reaches a peak a few hours later (Fig. 3), with the number of extensions then remaining constant for up to 24 h (not depicted). No significant differences in the induction of DC extensions were observed using invasive versus noninvasive strains of *Salmonella* in such experiments (Fig. 3). Collectively, these data suggest that many, if not most, DC trans-epithelial extensions arise as an active response to microbial products. As for the extensions seen in animals not treated with *Salmonella*, the extensions in infected mice were most frequent near the tip of the villi (not depicted).

MyD88–dependent signaling by diverse epithelial TLRs induces DC extension

Our observations and those reported previously suggested that pathogen-associated molecular pattern (PAMP) recognition might be directly or indirectly responsible for triggering DCs to extend processes across the epithelial cell layer. Both epithelial cells and DCs express TLRs that could mediate signaling in response to such material (16, 23, 24). Oral administration of peptidoglycan (PG), LPS, or CpGs (TLR2,

TLR4, and TLR9 ligands, respectively) was sufficient to induce DC protrusion in the terminal ileum, whereas the TLR3 ligand polyinosine-polycytidylic acid (poly(I:C); reference 25) and the TLR5 ligand flagellin (26) failed to do so (Fig. 4). These findings are in accord with evidence that TLR3 is not expressed on intestinal epithelial cells and that TLR5 is expressed at a very low level in the terminal part of the small intestine and may be predominantly present in lamina propria DCs (27, 28).

To study further the role of TLR signaling in triggering DC lumenal protrusions, we constructed three different bone marrow chimeras. The first was prepared using donor bone marrow from mice expressing CD11c-EGFP and recipients that were either wild-type or defective in TLR4 expression (29, 30). The second and the third chimeras were constructed using donor bone marrow from mice expressing MHC CII-EGFP (20) and recipients that were either defective in TLR2 or MyD88 expression (31, 32). After reconstitution, small bowel tissue from these mice was examined for DC extensions in the absence or presence of added TLR ligands.
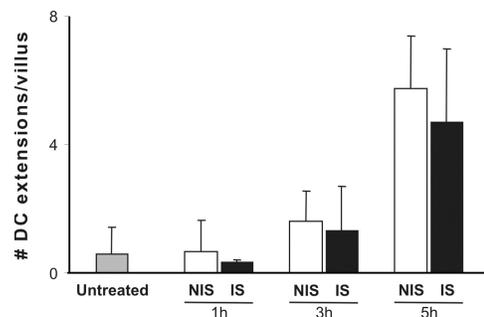
Figure 3. **Invasive and noninvasive *Salmonella* induce a similar number of DC extensions.** MHC CII-EGFP mice were treated orally with noninvasive (NIS; open bars) or invasive (IS; filled bars) *Salmonella* for 1, 3, or 5 h. The small intestine peri-cecal region was explanted and imaged, and the average number of DC extensions was calculated as described in Fig. 2. Data represent the average number of extensions ± SE/villus from >50 villi.
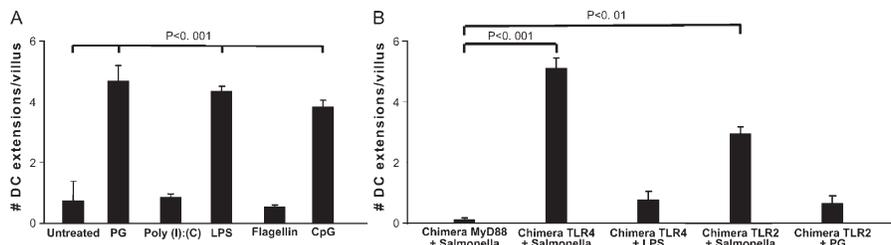
Figure 4. Role of epithelial TLRs and MyD88–dependent signaling in the induction of DC extensions. (A) Extensions of DCs across the small bowel epithelium were measured in MHC CII-EGFP animals as described in Fig. 2 either without treatment or after PG, poly(I:C), LPS, flagellin, or CpGs administration. (B) TLR4-, TLR2-, or MyD88-deficient recipient mice were irradiated and reconstituted with bone marrow cells from CD11c-EGFP (for TLR4-deficient recipients) or MHC CII-EGFP (for TLR2- and MyD88-deficient recipients) mice, respectively, to create CD11c-EGFP/TLR4$^{-/-}$, MHC CII-EGFP/TLR2$^{-/-}$, and MHC CII-EGFP/MyD88$^{-/-}$ bone marrow chimeras. The extensions of DCs across the small bowel epithelium were measured in these chimeric animals as described in Fig. 2 either without treatment or after noninvasive *Salmonella* gavage, as indicated. Data are represented as the average number of extensions $\pm$ SE/villus from two independent experiments for each chimera type.

Hosts with and without epithelial cell expression of either TLR2 or TLR4 had similar numbers of DC extensions in the proximal bowel regions that normally contained such processes. However, hosts lacking epithelial TLR4 did not show the induced appearance of such extensions in the peri–cecal region after administration of the TLR4 ligand LPS, even though the DCs in these animals expressed the receptor for LPS, whereas there was a significant increase in the number of such processes in control chimeras expressing TLR4 in nonhematopoietic cells (Fig. 4). Similarly, hosts lacking epithelial TLR2 did not show DC extensions in response to the TLR2 ligand PG in this segment of the small bowel, whereas control chimeras did (Fig. 4). Trans-epithelial projections from the DCs could be induced in both of these chimeras if noninvasive *Salmonella* organisms were administered, consistent with the diversity of potential TLR ligands produced by these bacteria and the ability of each of several TLR ligands to induce extensions when added individually (Fig. 4). Hosts lacking epithelial expression of MyD88 did not show DC extensions in response to *Salmonella* and had markedly fewer extensions in the absence of TLR ligand instillation or *Salmonella* infection (Fig. 4). These latter results suggest a possible minor role for the MyD88-independent pathway of TLR signaling (33, 34) or a very low baseline level of protrusion unrelated to TLR stimuli (Fig. 3). Overall, these results indicate that most DC extensions across the small bowel epithelium occur in response to MyD88-dependent TLR signaling via receptors expressed by the epithelial cells themselves and that distinct TLRs can independently mediate this effect upon ligand exposure.

Given the differences in distribution of DC extensions in previous studies of cells expressing EGFP under control of the CX3CR1 locus versus the present analyses using CD11c or MHC CII–regulated EGFP expression, we used this information on actively induced DC extension to probe the relationship between CX3CR1, CX3CL1, and *Salmonella*-induced DC extensions. Previous work described CX3CR1-deficient DCs as being unable to extend processes into the gut lumen, leading to the conclusion that CX3CL1-induced signaling was a necessary factor in this phenomenon (13, 19).

Using CX3CR1-EGFP homozygous mice deficient in CX3CR1 expression, we confirmed that there is no increase in the number of DCs sending projections into the terminal ileum upon *Salmonella* infection. Surprisingly, in the proximal ileum of these same mice, we detected a significant increase in DC projections (Fig. S2, available at http://www.jem.org/cgi/content/full/jem.20061884/DC1). These results indicate that DCs lacking CX3CR1 are nonetheless able to respond to signals evoked by inflammatory stimuli by sending processes across the bowel epithelium.

To study the role of CX3CL1 in DC protrusions, we used quantitative PCR to measure CX3CL1 mRNA levels in the small bowel tissue of mice given noninvasive *Salmonella* orally. No significant differences in the level of CX3CL1 mRNA were detected in the terminal ileum of infected as compared with uninfected mice, even though exposure to this bacterium evoked a strong DC extension response in this region of the small bowel as assessed using CD11C-EGFP or MHC CII-EGFP animals (Fig. S3, available at http://www.jem.org/cgi/content/full/jem.20061884/DC1, and Figs. 3 and 4). Given our finding that CX3CL1 mRNA levels did not change upon *Salmonella* infection, we examined whether any other chemokines known to affect DC behavior in the gut might be produced in a MyD88-dependent fashion in response to this stimulus. CCL20 is known to be produced by the intestinal epithelium in response to TLR stimuli (35). We therefore measured the level of mRNA for this chemokine in response to noninvasive *Salmonella* infection. An 18-fold increase in the level of CCL20 mRNA was measured in the terminal ileum of wild-type infected mice as compared with untreated mice (Fig. S3). MyD88-deficient mice did not show this increase in chemokine mRNA, in accord with the preceding data showing that such animals largely lacked trans-epithelial DC extensions and that in these animals extensions could not be induced by TLR ligands or *Salmonella*.

Collectively, these data suggest that CX3CL1 is not directly involved in actively induced DC protrusion across the intestinal epithelium in the terminal ileum and that DCs marked using CX3CR1-EGFP expression are either distinct
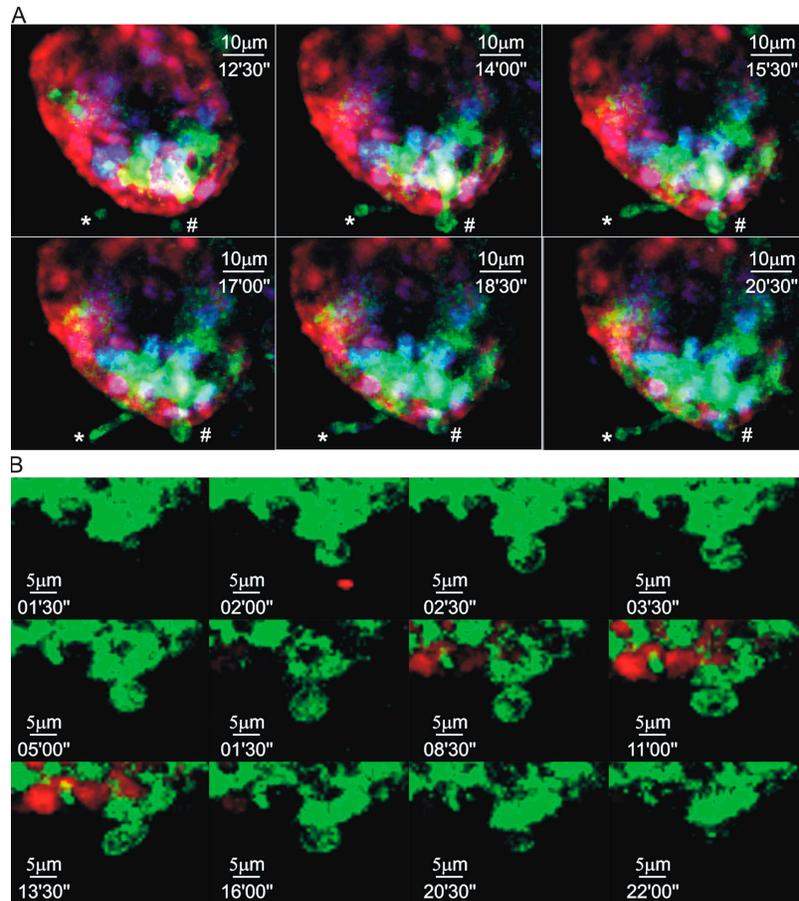
Figure 5. Characteristics of DC trans–epithelial extensions.
(A) MHC CII-EGFP mice were deprived of food for 4 h before oral *Salmonella* administration. The terminal ileum was then imaged by intravital two-photon microscopy. The nuclei of all the cells were labeled with Hoechst 33342 (blue), and the epithelium was stained with SNARF (red). Two different DCs can be seen extending dendritic processes into the intestinal lumen. In this example, both BB (#) and finger-like (*) dendritic extensions can be seen in the same villus (also see Video S3). (B) MHC CII-EGFP mice were deprived of food for 4 h before oral noninvasive *Salmonella* administration. The terminal ileal epithelium was then labeled with SNARF-1 (red) and imaged by two-photon microscopy. Sequential images from a time series are shown at high magnifications and reveal a dendrite reaching the luminal side and acquiring the BB shape. The protrusion is almost completely retracted after 22 min (see Video S4).

from or a subpopulation of those marked by CD11c-EGFP or MHC CII-EGFP labeling, potentially accounting for the different distribution of trans-epithelial extensions seen in previous studies as compared with the present investigation.

Dynamic visualization of the DC extension process

The demonstration that DC extensions could be actively induced by TLR signaling provided a method for capturing the process using four-dimensional (space and time) imaging methods. Explants from the peri-cecal small bowel region of animals expressing MHC CII-EGFP were imaged for up to 4 h using two-photon microscopy, using the red fluorescent dye carboxylic acid acetate succinimidyl ester (SNARF)-1 to counterstain the epithelial cells. Within 3 h of exposure of these explants to LPS or bacteria, the apical regions of villi in the peri-cecal region began to show the active emergence of DC processes across the epithelial layer. Although these were occasionally finger-like in appearance (Fig. 5 A and Video S3,

which is available at http://www.jem.org/cgi/content/full/jem.20061884/DC1), balloon-shaped structures dominated (Fig. 5 B and Videos S4 and S5). Once extended across the epithelium, the DC processes typically remained present for 10–40 min before being withdrawn.

In vitro data indicated that DC extension across a reconstituted epithelial cell layer occurred without disruption of the tight junction (17, 18). To examine if this was the case using normal tissue, fluorescent dextran was added to the medium bathing the explants. No accumulation of the exogenous dextran was seen in the lamina propria or in the DCs themselves (Fig. 6 and Video S5). This is consistent with the maintenance of the epithelial junctions and with limited macropinocytosis or micropinocytosis by the DC extensions.

Bacterial interaction with DC extensions

Previous work using in vitro models, tissue explants, and closed loop preparations demonstrated that DCs can capture

bacteria across an epithelial barrier (13, 17, 19). We confirmed these data using the previously described experimental model (17) and static imaging (unpublished data), and then conducted four-dimensional imaging in an attempt to characterize this process dynamically. Using both explant and intravital methods, it was possible to obtain rare images of DC BBs interacting with noninvasive *Salmonella* (36, 37) in the lumenal space (Fig. 7 A and Video S6, which is available at http://www.jem.org/cgi/content/full/jem.20061884/DC1) and BBs with a captured red *Salmonella* inside (Fig. 7 B and Video S7). However, the infrequent nature of these events (the total accumulation of noninvasive *Salmonella* after gavage was never >10–20 organisms per villus per 24 h), as well as rapid bleaching of the captured organisms, precluded direct visualization of binding and withdrawal of bacteria-containing processes into the lamina propria.

DISCUSSION

In this paper, we have used dynamic explant and intravital two-photon imaging to study trans-epithelial DC extension into the small bowel. Our data confirm and extend previous reports on the capacity of lamina propria DCs to send processes across the columnar epithelial layer without disruption of the tight junction between these cells and to interact with lumenal microbial flora (13, 17, 19). Most of the DC extensions showed an unusual spherical shape, and their frequency differed markedly along the length of the small bowel. In the more proximal small bowel segments in which the DC processes were numerous in normal uninfected animals, such extension appeared to reflect an active response to local commensal flora and bacterial products. The vast majority of such responses to endogenous bacteria and those occurring in the presence of exogenous species such as *Salmonella* involved MyD88-dependent signaling evoked by interaction of any of several epithelial TLRs with cognate microbial products.

Two previous studies reported the distribution of small bowel trans-epithelial extensions of lamina propria DCs, using static imaging based on expression of EGFP under the control of the CX3CR1 regulatory region (13, 19). In these reports, the highest frequency of such extensions was observed in the terminal ileum in mice of the C57BL/6 background, which were also used here. In marked contrast, we found that with a conventional gut flora, substantial numbers

of such processes are present in the proximal ileum and in the jejunum, with a concentration toward the apical region of the villi, but that only small numbers of such extensions are present in the terminal few centimeters of the ileum (the peri-cecal region) of these same mice. We obtained a similar result using two different reporter strains (MHC CII-EGFP and CD11c-EGFP). Furthermore, in contrast to what was observed by Niess et al. (19) using CX3CR1-EGFP$^{+/+}$ mice that are unresponsive to CX3CL1 (38), we were able to detect the presence in these mutant animals of trans-epithelial dendrites, but only in the proximal ileum of *Salmonella*-treated mice. At present, we do not have a definitive explanation for the difference between our findings and the results of these two previous studies. However, it may be important that our work involved imaging based on EGFP expression by what may be a much larger and potentially distinct fraction of DCs, based on control of the reporter by the CD11c (21) or MHC class II (20) gene regulatory regions. Given the absence of a measurable change in CX3CL1 mRNA expression in response to bacterial stimuli that potently induce DC extensions in the terminal ileum, and the induction of extensions in the proximal bowel of animals lacking CX3CR1 expression, these findings suggest that induced up-regulation of CX3CL1 does not play a direct role in the DC extension process, but that the absence of CX3CR1 may change the characteristics of the DCs resident in intestinal epithelium, perhaps altering the adhesive properties of these cells (39).

A primary focus of the present work was on control of the extension process. Treatment with broad-spectrum antibiotics to reduce the load of commensal organisms reduced the number of DC extensions seen in the jejunum and proximal ileum where the number of extensions was high in untreated, uninfected animals. This result suggested that active responses to microbial products contribute to the DC protrusion process, and in accord with this notion, the introduction of viable invasive or noninvasive *Salmonella* organisms induced DC trans-epithelial extensions in the terminal ileum (peri-cecal region) where these processes were rare in normal animals. One possible explanation for the low frequency of extensions in the pre-cecal region of normal mice is a higher level of defensin production in this site. This suggestion is in accord with the variation in protrusion frequency we observed along the length of an individual villus. It was low
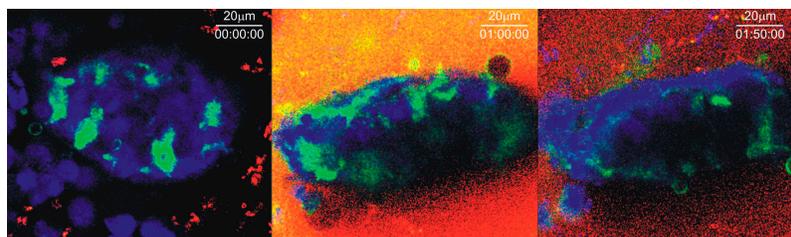

Figure 6.   Epithelial cell continuity is preserved during DC extension. Three sequential images of a villus in an ileal explant from an MHC CII-EGFP mouse given *Salmonella* orally and immersed in buffer containing TRITC-dextran showing the exclusion of the tracer from the basolateral surfaces of the epithelial layer (also see Video S5).
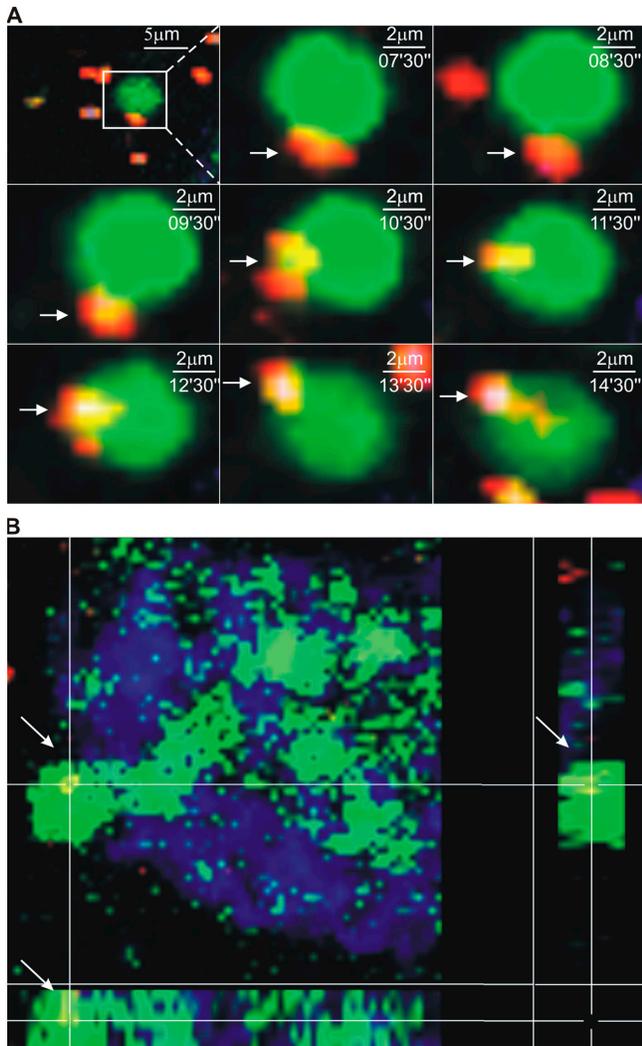
Figure 7. Interaction of inert particles and bacteria with DC extensions in the bowel lumen. (A) A time sequence of images from the same region of a villus in the terminal ileum of an MHC CII-EGFP mouse. The mouse was given noninvasive *Salmonella* (red) orally. A segment of the terminal ileum was isolated 5 h later, the epithelium was stained using Cell Tracker Blue, and the preparation was imaged by two-photon microscopy. A BB can be seen interacting with a fluorescent bacterium before internalizing it. (B) A three-dimensional section of a villus in the terminal ileum from an MHC CII-EGFP mouse. Noninvasive *Salmonella* (red) was given orally 5 h before the terminal ileum was explanted and stained with Cell Tracker Blue. A *Salmonella* bacterium just internalized by a DC extension with the typical BB shape is shown by the colocalization of green and red in the three-dimensional section (also see Videos S6 and S7).

near the crypts containing Paneth cells that produce high levels of defensins (40) and greater toward the apex where the antimicrobial mediators would be less abundant. Presumably, the high dose of bacteria administered was able to overcome local defense mechanisms that may otherwise limit the local availability of microbial stimuli able to induce DC extensions.

The evidence that DC protrusion could be influenced by bacterial load suggested a possible role in this process for signaling through receptors sensitive to microbial products. TLRs were the most likely candidates, and various TLRs are expressed on the apical surface of gut epithelium (41). In agreement with this notion, individual TLR ligands such as LPS (TLR4), PG (TLR2), or CpGs (TLR9) induced a substantial increase in the frequency of such extensions in the peri-cecal region, as did *Salmonella*. The TLR3 ligand poly (I:C) was not able to induce a change in DC extension frequency. This is consistent with the observation that TLR3 is not expressed by the intestinal epithelium. Intriguingly, flagellin, whose receptor is TLR5, was also unable to cause this response. This finding is in accord with recent studies that show a very low level or no expression of TLR5 by the epithelium of the ileum and with the ability of flagellin to induce a humoral response only after the disruption of epithelial continuity (27, 28, 42). Collectively, these data indicate that several but not all lumenal PAMPs can stimulate the intestinal epithelium to induce an extension response from lamina propria DCs.

Experiments using radiation chimeras showed that microbial products required signaling via TLRs expressed by nonhematopoietic (epithelial) cells to evoke the DC response, that engagement of any of several TLRs was sufficient, and that the signaling process was largely MyD88 dependent. Indeed, in nonchimeric MyD88-deficient mice, the number of DC extensions seen in the absence of added bacteria or PAMPS was reduced almost to zero. We have not yet been able to study directly the reciprocal issue of whether TLR signaling by the lamina propria DCs is also required for the extension process. However, the fact that lamina propria DCs have been reported not to express TLR4 (27), our observations that LPS alone can induce DC extensions, and the finding that bone marrow chimeras with TLR4 expression only on hematopoietic cells do not show DC extension in response to LPS suggest that the TLR signaling by epithelial cells is necessary and sufficient to induce the extension phenomenon.

The observation of robust MyD88-dependent induction of CCL20 transcription in the ilea of animals given noninvasive *Salmonella* provides further evidence for an active epithelial cell response to TLR engagement. Whether this chemokine plays any role in promoting DC extension is an open question at the moment. We have not detected an increased number of DCs in the terminal ileum at early times after *Salmonella* administration even though CCL20 has been reported to recruit DC precursors to the small bowel (14). Therefore, it is unlikely that CCL20 contributes to an acute increase in the number of DC extensions by enlarging the pool of DCs present in the lamina propria. A possible role for CCL20-dependent cell shape changes has not yet been ruled in or out by direct experiment.

In agreement with previous in vitro and static imaging studies (13, 17, 19), we find that DC extensions are able to interact with intralumenal microbial material. Our live imaging data clearly show the interaction of DC luminal BBs with

noninvasive labeled *Salmonella* (36, 37) for several minutes and the presence of bacteria in subepithelial DCs. At this time, we have no evidence that DC sampling is discriminatory. Both inert beads and either invasive or noninvasive bacteria are acquired well by lamina propria DCs based on analysis of static images, and both can be seen associating with DC extensions in live images (unpublished data). But it would be surprising if scavenger receptors, FcR, and C-type lectins did not define the preferred targets of the capture process (43). We have not yet been able to follow a DC with an internal microbial load leaving its sub-epithelial position and entering a lymphatic for migration to a local lymph node (44), migrating to a nearby Payer's patch to initiate a response in this site (45–48), or interacting with a memory T cell within the lamina propria. New methods for maintaining animal anesthesia for more prolonged periods, together with bacteria labeled with nonbleaching probes such as quantum dots (49), may allow both the capture process and the subsequent fate of the loaded DC to be visualized.

The spherical shape of the DC extensions (BBs) was unexpected. We cannot at present rule out that this is an artifact of the imaging method, perhaps due to removal of the mucus layer that typically covers the epithelial cell apical surface and that might constrain the shape of the DC protrusion. In a buffer-filled lumen, membranes moving past the end of the tight junction and lacking support from F-actin (unpublished data) may simply take the energetically most favorable shape, that of a sphere.

A characteristic feature of the immune system is the dynamic behavior of its constituent cells. The development of methods for high resolution intravital imaging of lymphoid (50, 51) and other tissue sites (52–55) has begun to reveal how immune cells move, interact, and respond in situ, adding to our understanding of normal and pathological immune events. Our visualization here of active DC extension into the small bowel lumen and the description of the first steps in the signaling cascade controlling this process provide a clear example of the utility of this new technology in adding to the insights already generated from more conventional analyses of this important host–pathogen interface.

MATERIALS AND METHODS

Animals. CD11c-EGFP transgenic mice (21), CX3CR1-EGFP mice (38), TLR2-deficient mice (31), and TLR4-deficient mice (29, 30) were obtained from The Jackson Laboratory. MHC CII-EGFP knock-in mice (line 270 on a RAG-2$^{-/-}$ background; reference 20) were produced at Taconic Farms from breeding stock provided by H. Ploegh (Harvard Medical School, Boston, MA). MyD88–deficient mice (32) were provided by S. Akira (Osaka University, Osaka, Japan). CX3CR1-EGFP mice on a BALB/c background were provided by B. Graham and T. Johnson (Vaccine Research Center, NIAID, NIH). All other animals were on the C57BL/6 background, and all mice were housed and handled according to NIH institutional guidelines under an approved animal protocol.

Intestinal DC purification. Intestinal tissue from killed line 270 CD11c-EGFP mice was opened longitudinally and washed several times in PBS. The tissue was cut into 1-cm pieces, and these fragments were incubated at 37°C on a shaking platform with 145 μg/ml DTT and 0.37 mg/ml EDTA in PBS for 15 min. The tissue was then washed several times in 145 μg/ml DTT in

PBS, and then digested in RPMI 1640 containing 0.15 mg/ml type II collagenase (Worthington) and 0.1 mg/ml DNase (Roche Molecular Biochemicals) for 60 min at 37°C on a shaking platform. The released cells were enriched by 25% Percoll gradient (Sigma-Aldrich), stained with anti–CD11c-APC, and analyzed by flow cytometry.

Construction of bone marrow chimeras. 3–5-wk-old TLR4- or TLR2-deficient recipient mice were sublethally irradiated with 900 rads, whereas MyD88-deficent recipient mice were irradiated with 500 rads. On the same day, 5×10^4 bone marrow cells from CD11c-EGFP or MHC CII-EGFP mice were harvested and infused into TLR4-deficient or into TLR2- or MyD88-deficient irradiated recipient mice via the tail vein, respectively, to create CD11c-EGFP/TLR4$^{-/-}$, MHC CII-EGFP/TLR2$^{-/-}$, or MHC CII-EGFP/MyD88$^{-/-}$ bone marrow chimeras. These mice were kept in isolators and provided neomycin-containing water until use 8–10 wk later.

Reagents. RPMI 1640 medium without phenol red was purchased from Biosource International. LPS (*Escherichia coli* serotype 026:B6) and TRITC-dextran (160,000 mw) were obtained from Sigma-Aldrich. Poly(I:C) was obtained from GE Healthcare. CpGs (GCTAGACGTTAGGT and TCAAC-GTTGA; reference 56) were synthesized at the Facility for Biotechnology Resources at the NIH. Fluorescent beads (Fluorobrite polychromatic red; 1-μm microspheres) were obtained from Polysciences, Inc. Anti–mouse CD11c mAb labeled with APC was purchased from BD Biosciences.

Bacterial strains and oral administration. Unless otherwise stated, all in vivo experiments involved the administration of attenuated *Salmonella typhimurium* deficient in both the SP-1 (*InvA*-) and SP-2 (*ssaV*) genes, conferring the invasive phenotype and the capacity for intraphagosomal survival, respectively (36, 37). In selected experiments, the invasive *S. typhimurium* strain SL1344 (57) was also used. A recombinant red fluorescent variant of each strain was generated by expressing the red fluorescent protein DsRed under the transcriptional control of the *LacZ* promoter. These bacterial strains were grown as described previously (58). Preparation and feeding of mice with bacteria was performed with 200 μl (10%, wt/vol) NaHCO$_3$ given 10 min before 200 μl of bacterial suspension (2×10^9 bacteria in PBS) or 1 mg/ml LPS or 1 mg/ml PG. Mice were deprived of food for 4 h before and 1 h after oral treatment, which was performed using an animal feeding needle.

Antibiotic treatment. For experiments involving the effect of normal gut flora on luminal DC projections, we included 5 mg/ml ampicillin, 3 mg/ml kanamycin, and 5 mg/ml neomycin in the drinking water for 5 d before analysis.

Real-time quantitative RT-PCR. Ileal samples were collected 2 cm above the cecum, the luminal content was carefully washed out, and total RNA was extracted using the RNeasy Mini kit Protocol (QIAGEN). cDNA was synthesized from ∼1 μg total RNA using the SuperScript III First-Strand Synthesis System for RT-PCR (Invitrogen) according to the manufacturer's protocol. Expression levels of CCL20, CX3CL1, and GAPDH mRNA were measured by quantitative PCR based on the manufacturer's recommended protocol with the TaqMan Universal PCR Master Mix, followed by analysis on an ABI7900 (Applied Biosystems). Triplicate reactions were performed for each cDNA preparation. Data were expressed as 2$^{\Delta\Delta CT}$ relative to GAPDH levels in each sample.

Explant preparation. Mice were deprived of food for 4 h before and, in the case of administration of bacteria or LPS, 1 h after these procedures before being killed by CO$_2$ asphyxiation. The intestine was then removed surgically, and the region of interest was immediately everted and washed twice with PBS at 37°C. The epithelium was stained using 20 μM SNARF or 100 ng/ml Cell Tracker Blue (both from Invitrogen) for 3 min at 37°C in PBS. The everted intestinal segment was then immobilized on the surface of a Petri dish using Vetbond epoxy glue (3M Animal Care Products) and a mechanical support, and the entire preparation was submerged with 20 ml of

phenol red–free RPMI maintained at 37°C within a custom microscope enclosure fitted with both an environmental heater and a thermal blanket. Experiments conducted with and without the use of medium superfused with a gas mixture of 95% O_2/5% CO_2 gave similar results.

Intravital preparation for microscopy. Mice were anesthetized using nebulized isofluorane (2% induction, 1% maintenance) in 30% O_2/68–69% air. The abdomen was shaved, and a vertical incision was performed at the cecal level to reveal the terminal ileum. The terminal 7–8 cm of the small intestine was externalized from the peritoneum while carefully preserving blood flow and lymphatic vessel continuity. The region of interest was then immobilized on the disposable stage by using both a solid support and Vet-bond tissue adhesive. The lumen was surgically exposed using a battery-operated cautery (AARON Medical) and washed several times with PBS at 37°C to remove fecal material and mucus from lumenal surfaces. The epithelial surface was then stained with 200 µl SNARF diluted in 20 µM PBS at 37°C for 3 min. In some cases nuclei were stained blue using Hoechst 33342. After washing with PBS at 37°C, the exposed region of the bowel was bathed in phenol red–free RPMI 1640 at 37°C, and the whole animal was placed within an enclosed microscope stage fitted with both an environmental heater and a thermal blanket.

Two-photon microscopy. Two-photon microscopy was conducted using a Bio-Rad Laboratories/Carl Zeiss MicroImaging, Inc. Radiance 2100MP system equipped with a Nikon 600FN upright microscope, 20× water immersion lens (N.A. 0.95; Olympus), and either a Mira 900 Sa:Ti femtosecond-pulsed laser driven by a 10-W Verdi pump laser (Coherent) or a Chameleon laser (Coherent) with similar specifications, both tuned to 880 nm. The typical pixel size of the image field was 1.09 µm, and the x-y dimensions of the scan area were 560 × 560 µm. The typical optical z-step size was 1.5 µm. Serial x-y images were collected over the entire z depth every 30–60 s, and the entire process was repeated for up to 120 min to obtain a four-dimensional dataset.

Topographic analysis of BBs. The terminal part of the ileum from MHC CII-EGFP mice was surgically removed, immediately everted, and stained using 20 µM SNARF-1. Two-photon microscopy at 880 nm using the imaging conditions described above was then used to collect high resolution static images of complete villi starting from the tips and ending at the bases. The number of protrusions (BBs) in an x-y image at a particular z-step and the total number of z-step images (ZTot) from the tip to base of the villus were recorded. Each villus was arbitrarily subdivided into 10 equal-sized compartments from the bottom to the apical region. Relative BB positions were then calculated using the following equation: BB = ZBB × 100 / ZTot. The numbers of DC extensions per villus were expressed as mean ± SE.

Regional BB distribution. The small intestine was explanted and subdivided in six 5-cm segments. Each segment was everted, stained with SNARF, and immobilized on a Petri dish as described previously. Two-photon microscopy was then used to acquire images of randomly selected areas within these small intestine segments. The number of DC extensions was determined by inspection of each z-slice in image stacks collected at multiple sites within the indicated subregions of the small bowel.

Epithelial cell continuity detection. The explants were prepared as described previously. During image acquisition, 200 µl of 10 mg/ml TRITC Dextran in PBS was added to the medium in the Petri dish, and imaging continued.

Image processing. Datasets were processed using edge-preserving filters for the green channel and a median filter for the red and blue channels (Bitplane, 4.2; Imaris) to denoise the images. The same software was used to color balance the images, with all manipulations of color and intensity applied equally to an entire image stack, and the resulting files used create two-dimensional maximum intensity projections for the image stack corresponding to each time segment. These projections were then combined using Adobe After Effects to generate video sequences. The rate enhancements of these videos relative to real time are indicated in the legends.

Statistics. All data were expressed as average values of experimental data points, and SEs were determined using the calculated standard deviation of a dataset divided by the number of data points within each dataset. p-values for the comparison of two data samples were obtained using the two-tailed Student's *t* test.

Online supplemental material. Fig. S1 shows that MHC class II–EGFP cells are CD11c^{+}. Fig. S2 shows the presence of DC extensions in the lumen of a CX3CR1^{+/+} EGFP mouse. Fig. S3 shows CCL20 production by epithelial cells in response to *Salmonella*. Videos S1 and S2 show reconstructions of DC extensions across the epithelial layer of the terminal ileum. Video S3 shows different shapes of the extensions through the epithelium. Video S4 shows a dendrite reaching the luminal side and acquiring the BB shape. Video S5 shows that epithelial cell continuity is preserved during DC extension. Videos S6 and S7 show DC extensions that capture fluorescent *Salmonella*. The online supplemental material is available at http://www.jem.org/cgi/content/full/jem.20061884/DC1.

REFERENCES

1. Pasare, C., and R. Medzhitov. 2003. Toll pathway-dependent blockade of CD4+CD25+ T cell-mediated suppression by dendritic cells. *Science*. 299:1033–1036.

2. Rakoff-Nahoum, S., J. Paglino, F. Eslami-Varzaneh, S. Edberg, and R. Medzhitov. 2004. Recognition of commensal microflora by toll-like receptors is required for intestinal homeostasis. *Cell*. 118:229–241.

3. Ganz, T. 2003. Defensins: antimicrobial peptides of innate immunity. *Nat. Rev. Immunol*. 3:710–720.

4. Lamm, M.E. 1997. Interaction of antigens and antibodies at mucosal surfaces. *Annu. Rev. Microbiol*. 51:311–340.

5. Macpherson, A.J., D. Gatto, E. Sainsbury, G.R. Harriman, H. Hengartner, and R.M. Zinkernagel. 2000. A primitive T cell-independent mechanism of intestinal mucosal IgA responses to commensal bacteria. *Science*. 288:2222–2226.

6. Wykes, M., A. Pombo, C. Jenkins, and G.G. MacPherson. 1998. Dendritic cells interact directly with naive B lymphocytes to transfer antigen and initiate class switching in a primary T-dependent response. *J. Immunol*. 161:1313–1319.

7. MacPherson, G., N. Kushnir, and M. Wykes. 1999. Dendritic cells, B cells and the regulation of antibody synthesis. *Immunol. Rev*. 172:325–334.

8. Macpherson, A.J., and T. Uhr. 2004. Induction of protective IgA by intestinal dendritic cells carrying commensal bacteria. *Science*. 303:1662–1665.

9. Qi, H., J.G. Egen, A.Y. Huang, and R.N. Germain. 2006. Extrafollicular activation of lymph node B cells by antigen-bearing dendritic cells. *Science*. 312:1672–1676.

10. Neutra, M.R., N.J. Mantis, A. Frey, and P.J. Giannasca. 1999. The composition and function of M cell apical membranes: implications for microbial pathogenesis. *Semin. Immunol*. 11:171–181.

11. Iwasaki, A., and B.L. Kelsall. 2001. Unique functions of CD11b+, CD8 alpha+, and double-negative Peyer's patch dendritic cells. *J. Immunol*. 166:4884–4890.

12. Jang, D.H., J.H. Han, S.H. Lee, Y.S. Lee, H. Park, S.H. Lee, H. Kim, and B.K. Kaang. 2005. Cofilin expression induces cofilin-actin rod formation and disrupts synaptic structure and function in Aplysia synapses. *Proc. Natl. Acad. Sci. USA*. 102:16072–16077.

13. Vallon-Eberhard, A., L. Landsman, N. Yogev, B. Verrier, and S. Jung. 2006. Transepithelial pathogen uptake into the small intestinal lamina propria. *J. Immunol*. 176:2465–2469.

14. Strober, W., B. Kelsall, I. Fuss, T. Marth, B. Ludviksson, R. Ehrhardt, and M. Neurath. 1997. Reciprocal IFN-gamma and TGF-beta responses regulate the occurrence of mucosal inflammation. *Immunol. Today*. 18:61–64.

15. Powrie, F., J. Carlino, M.W. Leach, S. Mauze, and R.L. Coffman. 1996. A critical role for transforming growth factor β but not interleukin 4 in the suppression of T helper type 1–mediated colitis by CD45RB(low) CD4+ T cells. *J. Exp. Med*. 183:2669–2674.

16. Rimoldi, M., M. Chieppa, P. Larghi, M. Vulcano, P. Allavena, and M. Rescigno. 2005. Monocyte-derived dendritic cells activated by bacteria or by bacteria-stimulated epithelial cells are functionally different. *Blood*. 106:2818–2826.

17. Rescigno, M., M. Urbano, B. Valzasina, M. Francolini, G. Rotta, R. Bonasio, F. Granucci, J.P. Kraehenbuhl, and P. Ricciardi-Castagnoli. 2001. Dendritic cells express tight junction proteins and penetrate gut epithelial monolayers to sample bacteria. *Nat. Immunol*. 2:361–367.

18. Rescigno, M., G. Rotta, B. Valzasina, and P. Ricciardi-Castagnoli. 2001. Dendritic cells shuttle microbes across gut epithelial monolayers. *Immunobiology*. 204:572–581.

19. Niess, J.H., S. Brand, X. Gu, L. Landsman, S. Jung, B.A. McCormick, J.M. Vyas, M. Boes, H.L. Ploegh, J.G. Fox, et al. 2005. CX3CR1-mediated dendritic cell access to the intestinal lumen and bacterial clearance. *Science*. 307:254–258.

20. Boes, M., J. Cerny, R. Massol, M. Op den Brouw, T. Kirchhausen, J. Chen, and H.L. Ploegh. 2002. T-cell engagement of dendritic cells rapidly rearranges MHC class II transport. *Nature*. 418:983–988.

21. Jung, S., D. Unutmaz, P. Wong, G. Sano, K. De los Santos, T. Sparwasser, S. Wu, S. Vuthoori, K. Ko, F. Zavala, et al. 2002. In vivo depletion of CD11c(+) dendritic cells abrogates priming of CD8(+) T cells by exogenous cell-associated antigens. *Immunity*. 17:211–220.

22. Ruedl, C., C. Rieser, G. Bock, G. Wick, and H. Wolf. 1996. Phenotypic and functional characterization of CD11c+ dendritic cell population in mouse Peyer's patches. *Eur. J. Immunol*. 26:1801–1806.

23. Cario, E. 2005. Bacterial interactions with cells of the intestinal mucosa: Toll-like receptors and NOD2. *Gut*. 54:1182–1193.

24. Hemmi, H., O. Takeuchi, T. Kawai, T. Kaisho, S. Sato, H. Sanjo, M. Matsumoto, K. Hoshino, H. Wagner, K. Takeda, and S. Akira. 2000. A Toll-like receptor recognizes bacterial DNA. *Nature*. 408:740–745.

25. Alexopoulou, L., A.C. Holt, R. Medzhitov, and R.A. Flavell. 2001. Recognition of double-stranded RNA and activation of NF-kappaB by Toll-like receptor 3. *Nature*. 413:732–738.

26. Hayashi, F., K.D. Smith, A. Ozinsky, T.R. Hawn, E.C. Yi, D.R. Goodlett, J.K. Eng, S. Akira, D.M. Underhill, and A. Aderem. 2001. The innate immune response to bacterial flagellin is mediated by Toll-like receptor 5. *Nature*. 410:1099–1103.

27. Uematsu, S., M.H. Jang, N. Chevrier, Z. Guo, Y. Kumagai, M. Yamamoto, H. Kato, N. Sougawa, H. Matsui, H. Kuwata, et al. 2006. Detection of pathogenic intestinal bacteria by Toll-like receptor 5 on intestinal CD11c(+) lamina propria cells. *Nat. Immunol*. 7:868–874.

28. Ortega-Cava, C.F., S. Ishihara, M.A. Rumi, M.M. Aziz, H. Kazumori, T. Yuki, Y. Mishima, I. Moriyama, C. Kadota, N. Oshima, et al. 2006. Epithelial toll-like receptor 5 is constitutively localized in the mouse cecum and exhibits distinctive down-regulation during experimental colitis. *Clin. Vaccine Immunol*. 13:132–138.

29. Vogel, S.N., C.T. Hansen, and D.L. Rosenstreich. 1979. Characterization of a congenitally LPS-resistant, athymic mouse strain. *J. Immunol*. 122:619–622.

30. Beutler, B., X. Du, and A. Poltorak. 2001. Identification of Toll-like receptor 4 (Tlr4) as the sole conduit for LPS signal transduction: genetic and evolutionary studies. *J. Endotoxin Res*. 7:277–280.

31. Wooten, R.M., Y. Ma, R.A. Yoder, J.P. Brown, J.H. Weis, J.F. Zachary, C.J. Kirschning, and J.J. Weis. 2002. Toll-like receptor 2 is required for innate, but not acquired, host defense to Borrelia burgdorferi. *J. Immunol*. 168:348–355.

32. Adachi, O., T. Kawai, K. Takeda, M. Matsumoto, H. Tsutsui, M. Sakagami, K. Nakanishi, and S. Akira. 1998. Targeted disruption of the MyD88 gene results in loss of IL-1- and IL-18-mediated function. *Immunity*. 9:143–150.

33. Janssens, S., K. Burns, J. Tschopp, and R. Beyaert. 2002. Regulation of interleukin-1- and lipopolysaccharide-induced NF-kappaB activation by alternative splicing of MyD88. *Curr. Biol*. 12:467–471.

34. Burns, K., S. Janssens, B. Brissoni, N. Olivos, R. Beyaert, and J. Tschopp. 2003. Inhibition of interleukin 1 receptor/Toll-like receptor signaling through the alternatively spliced, short form of MyD88 is due to its failure to recruit IRAK-4. *J. Exp. Med*. 197:263–268.

35. Izadpanah, A., M.B. Dwinell, L. Eckmann, N.M. Varki, and M.F. Kagnoff. 2001. Regulated MIP-3alpha/CCL20 production by human intestinal epithelium: mechanism for modulating mucosal immunity. *Am. J. Physiol. Gastrointest. Liver Physiol*. 280:G710–G719.

36. Galan, J.E., and R. Curtiss III. 1989. Cloning and molecular characterization of genes whose products allow Salmonella typhimurium to penetrate tissue culture cells. *Proc. Natl. Acad. Sci. USA*. 86:6383–6387.

37. Shea, J.E., C.R. Beuzon, C. Gleeson, R. Mundy, and D.W. Holden. 1999. Influence of the Salmonella typhimurium pathogenicity island 2 type III secretion system on bacterial growth in the mouse. *Infect. Immun*. 67:213–219.

38. Jung, S., J. Aliberti, P. Graemmel, M.J. Sunshine, G.W. Kreutzberg, A. Sher, and D.R. Littman. 2000. Analysis of fractalkine receptor CX(3)CR1 function by targeted deletion and green fluorescent protein reporter gene insertion. *Mol. Cell. Biol*. 20:4106–4114.

39. Fong, A.M., L.A. Robinson, D.A. Steeber, T.F. Tedder, O. Yoshie, T. Imai, and D.D. Patel. 1998. Fractalkine and CX3CR1 mediate a novel mechanism of leukocyte capture, firm adhesion, and activation under physiologic flow. *J. Exp. Med*. 188:1413–1419.

40. Ayabe, T., T. Ashida, Y. Kohgo, and T. Kono. 2004. The role of Paneth cells and their antimicrobial peptides in innate host defense. *Trends Microbiol*. 12:394–398.

41. Chabot, S., J.S. Wagner, S. Farrant, and M.R. Neutra. 2006. TLRs regulate the gatekeeping functions of the intestinal follicle-associated epithelium. *J. Immunol*. 176:4275–4283.

42. Sanders, C.J., Y. Yu, D.A. Moore III, I.R. Williams, and A.T. Gewirtz. 2006. Humoral immune response to flagellin requires T cells and activation of innate immunity. *J. Immunol*. 177:2810–2818.

43. Allavena, P., M. Chieppa, P. Monti, and L. Piemonti. 2004. From pattern recognition receptor to regulator of homeostasis: the double-faced macrophage mannose receptor. *Crit. Rev. Immunol*. 24:179–192.

44. Huang, F.P., N. Platt, M. Wykes, J.R. Major, T.J. Powell, C.D. Jenkins, and G.G. MacPherson. 2000. A discrete subpopulation of dendritic cells transports apoptotic intestinal epithelial cells to T cell areas of mesenteric lymph nodes. *J. Exp. Med*. 191:435–444.

45. Iwasaki, A., and B.L. Kelsall. 1999. Freshly isolated Peyer's patch, but not spleen, dendritic cells produce interleukin 10 and induce the differentiation of T helper type 2 cells. *J. Exp. Med*. 190:229–239.

46. Kelsall, B.L., and M. Rescigno. 2004. Mucosal dendritic cells in immunity and inflammation. *Nat. Immunol*. 5:1091–1095.

47. Alpan, O., E. Bachelder, E. Isil, H. Arnheiter, and P. Matzinger. 2004. 'Educated' dendritic cells act as messengers from memory to naive T helper cells. *Nat. Immunol*. 5:615–622.

48. Alpan, O., G. Rudomen, and P. Matzinger. 2001. The role of dendritic cells, B cells, and M cells in gut-oriented immune responses. *J. Immunol*. 166:4843–4852.

49. Larson, D.R., W.R. Zipfel, R.M. Williams, S.W. Clark, M.P. Bruchez, F.W. Wise, and W.W. Webb. 2003. Water-soluble quantum dots for multiphoton fluorescence imaging in vivo. *Science*. 300:1434–1436.

50. von Andrian, U.H., and T.R. Mempel. 2003. Homing and cellular traffic in lymph nodes. *Nat. Rev. Immunol*. 3:867–878.

51. Cahalan, M.D., I. Parker, S.H. Wei, and M.J. Miller. 2002. Two-photon tissue imaging: seeing the immune system in a fresh light. *Nat. Rev. Immunol.* 2:872–880.

52. Huang, A.Y., H. Qi, and R.N. Germain. 2004. Illuminating the landscape of in vivo immunity: insights from dynamic in situ imaging of secondary lymphoid tissues. *Immunity.* 21:331–339.

53. Germain, R.N., F. Castellino, M. Chieppa, J.G. Egen, A.Y. Huang, L.Y. Koo, and H. Qi. 2005. An extended vision for dynamic high-resolution intravital immune imaging. *Semin. Immunol.* 17:431–441.

54. Bousso, P., and E.A. Robey. 2004. Dynamic behavior of T cells and thymocytes in lymphoid organs as revealed by two-photon microscopy. *Immunity.* 21:349–355.

55. Germain, R.N., M.J. Miller, M.L. Dustin, and M.C. Nussenzweig. 2006. Dynamic imaging of the immune system: progress, pitfalls and promise. *Nat. Rev. Immunol.* 6:497–507.

56. Klinman, D.M. 2004. Immunotherapeutic uses of CpG oligodeoxynucleotides. *Nat. Rev. Immunol.* 4:249–258.

57. Gots, R.E., S.B. Formal, and R.A. Giannella. 1974. Indomethacin inhibition of Salmonella typhimurium, Shigella flexneri, and cholera-mediated rabbit ileal secretion. *J. Infect. Dis.* 130:280–284.

58. Avogadri, F., C. Martinoli, L. Petrovska, C. Chiodoni, P. Transidico, V. Bronte, R. Longhi, M.P. Colombo, G. Dougan, and M. Rescigno. 2005. Cancer immunotherapy based on killing of Salmonella-infected tumor cells. *Cancer Res.* 65:3920–3927.